Synthesis and Study Implications of Including Cobalt Oxide Nanoparticles on Structural and Optical Properties of Polyvinyl Alcohol Polyacrylic Acid Blend Films

Yaqoub Yousif Mahmood and Yaqoob Mohammed Jawad
Department of Physics, College of Science, University of Diyala, 32001 Baqubah, Diyala, Iraq
yawop111@gmail.com [1] , *Yaqoob.phys@uodiyala.edu.iq* [2]

Keywords: PVA, PAA , CoO NPs, Structural , Optical Analysis.

Abstract: Poly Vinyl Alcohol / Poly Acrylic Acid (PVA/PAA) pure polymeric films made using the solution casting technique , It is strengthened by cobalt oxide nanoparticles (CoONPs) through deposition approach at calcination temperatures (800 Cº), In different weight percentages ((pure,1,3,5,7and 9) % wt.), burned at different temperatures (800 Cº). XRD analysis of the as-synthesized nanomaterial powder indicated that cobalt oxide nanoparticles were obtained at the calcination temperature (800 C°). Heat treatment promotes continued crystallization, leading to an expansion in the dimensions of nanoparticles. The electron microscopy FESEM outcomes showed that the PVA/PAA polymeric film seems uniform and monolithic, and once used (PVA/ PAA:CoO 7 %) , It forms widely distributed agglomerates within nanocomposite membranes. Show The FTIR picture CoONPs don't negatively impact the structure of polymers. No covalent connections exist between PVA , PAA and CoONPs. The visual characteristics of the films reinforced with CoO nanoparticles demonstrate their influence on optical transmittance over the (200-1100) nm wavelength range, alongside a decline in energy band gap values from 5.07 eV to 4.68 eV .

1 INTRODUCTION

Recent years have witnessed great interest in researching and enhancing polymer mixtures to increase the properties of polymeric materials [1], [2]. Polymer mixtures consist of combining two or more types of polymers to create a novel substance with specialized characteristics. Polymer fusion facilitates the combination of beneficial properties from multiple polymers. [3], [4]. The primary benefits of polymer blends are customization of mechanical strength, thermal properties, melting stages, permeability and processability [5]. Hybrid materials that include a mixture of polymers and inorganic nanofillers are known as polymer-blended nanocomposites [6]. Nanoparticles of metals, oxides, clays, silica, carbon nanotubes, and graphene are among the most common inorganic nanofillers [7]. Polymer mixtures with nanofillers, such as metal oxide-based nanocomposites, show significant improvements in strength, stability, and barrier capabilities. These nanocomposites have opened up new opportunities for the use of high-quality materials in diverse applications [8], [9]. Cobalt (Co) is one of the transition elements in the periodic table with atomic number 27. It is a shiny, silver-gray metallic element, solid but brittle and does not exist in nature as a free metal. Cobalt is generally found in ores. Cobalt is a ferromagnetic material, self-magnetizing, stable in air, affected by dilute acids and not affected by water. Cobalt is a chemically active element as it is characterized by its ease of integration with other elements, forming many compounds such as salts and oxides. The most common water-soluble synthetic polymer made worldwide is polyvinyl alcohol (PVA) [10]. The tangible properties of PVA depend Upon its preparation method, which involves Polyvinyl acetate hydrolysis or partial hydrolysis [11]. Because PVA is a polymer obtained through hydrolysis, it has particularly remarkable properties compared to other thermoplastics. Synthetic PVA is a polymer that dissolves in water. Its outstanding mechanical qualities, high chemical resistance, and ease of preparation make it a popular choice for biomaterial applications [12]. A biodegradable, water-soluble polymer with a variety of industrial uses is polyacrylic acid (PAA). PVA is a polyacrylic acid-based polymer; it is used as an oral suspension and

bioadhesive. It is also used as a gelling and suspending agent and emulsion stabilizer [13], [14]. The aim of this research is to synthesis of cobalt oxide nanoparticles and include cobalt oxide nanoparticles to improve the PVA/PAA blend polymer's structural and optical characteristics. The results we obtained are consistent with the results of the researcher (Khader Abbas Daoud) and his group [15].

2 EXPERIMENTAL PART

2.1 Preparation of CoONPs

The synthesis of CoO NPs, or cobalt oxide nanoparticles was performed using the chemical precipitation approach [14]. The desired cobalt nitrate concentration was $Co(NO_3)_2.6H_2O$, with a molecular weight of 291.04 g/mol. Dissolve 29.103g of cobalt nitrate, $Co(NO_3)_2.6H_2O$, in 100ml of water that has been distilled. Stir the mixture utilizing a magnetic stirring device at 50 C° until A uniform mixture was obtained. Gradually add 25% ammonium hydroxide (NH_4OH) solution, and a precipitate was formed. The precipitate was cleaned. dried in an oven after being repeatedly rinsed with distilled water at 200 C° . The resulting precipitate went into a crucible and calcined at 800C° to obtain cobalt oxide nanoparticles (CoO NPs).

2.2 Creating Nanocomposites of PVA/PAA:CoO

Pure blend of PVA and PAA polymer and polymers Samples of nanocomposite were made using a straightforward technique “solution casting”. The blend film PVA/PAA has been prepared by mixture PVA (70%) and PAA (30%). To prepared PVA/PAA/CoO nanocomposites films with varying percentages of weight (pure, 1, 3, 5, 7, and 9) , by added 0.5 gm of cobalt oxide nanoparticale to 30 ml of distilled water [16].

2.3 Equations Used

The crystal size of the samples is is computed using the highest XRD peak utilizing Scherrer's equation as shown in (1) [17].

$$D = \frac{0.9\,\lambda}{\beta\, cos\theta} \ . \qquad (1)$$

The coefficient of absorption (α) was determined by applying (2) [18].

$$\alpha = 2.303\frac{A}{t} \ . \qquad (2)$$

The disparity in energy (Eg) value of the electronic transition that occurs indirectly was measured according to pure (3) [19].

$$\alpha h\boldsymbol{\nu} = P(h\boldsymbol{\nu} - E_g) \ . \qquad (3)$$

The refractive index and extinction index (no, ko) values were estimated using (4) and (5) [20], [21].

$$n_o = \left[\left(\frac{1+R}{1-R}\right)^2 - (k_o^2 + 1)\right]^{1/2} + \frac{1+R}{1-R} . \qquad (4)$$

$$k_\circ = \alpha\lambda/4\pi \ . \qquad (5)$$

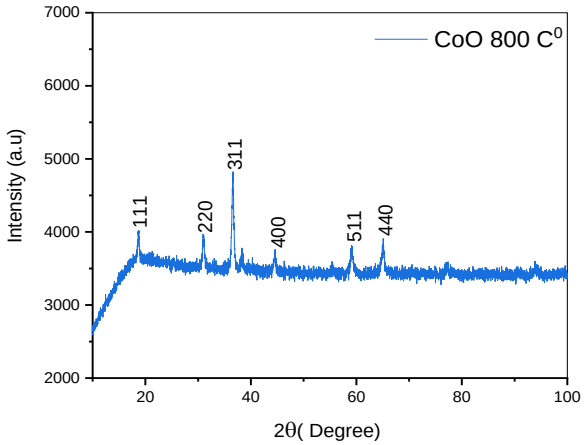

Figure 1: XRD patterns of prepared CoO NPs 800C° .

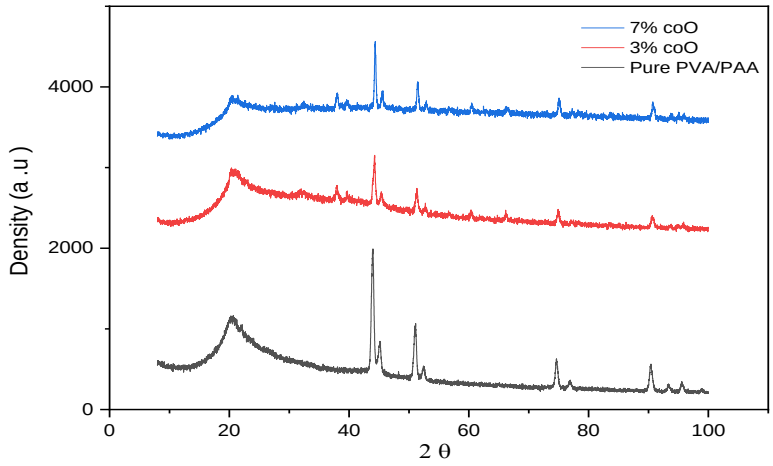

Figure 2: The XRD patterns obtained for pure (PVA/PAA) polymer films doped with CoO nanoparticles at weight ratios (3%, 7%).

3 RESULTS AND DISCUSSION.

3.1 Structural Analysis

3.1.1 X-Ray Diffraction (XRD)

The XRD test has been used to done to investigate the structure type (phase) and the crystalline size of prepared CoO NPs using the chemical precipitation method. Figure 1 presents the obtained XRD patterns of prepared CoO NPs.

After calcination of CoO nanoparticles at temperatures (800C°), several characteristic peaks were observed at (2θ = 19.001°, 31.27°, 36.84°, 44.81°, 59.35°, and 65.23°) of (111), (200), (311), (400), (511), and (440). The detected characteristic peaks confirmed the formation of cubic structure of CoO nanoparticles with stereogenic group (Fd3m No. 227) and lattice parameters (a = 8.1290 Aº, b = 8.1290 A°, c = 8.1290 A°) and (α = β = γ = 90°) which are consistent with the usual data (ICDD). (00-043-1003) [14].

Table 1: Calculated XRD parameter of synthesized CoO NPs 800Cº.

Sample	CoO NPs at 800 °C
2θ (°) Standard	36.83
2θ (°) Practical	36.53
FWHM (deg)	0.4149
D (nm)	20.16
(hkl)	(311)

XRD test was conducted for pure (PVA/PAA) polymer films doped with CoO nanoparticles at weight ratios (3%, 7%). It was found that the peaks of the doped (PVA/PAA) polymer films increased in intensity and became sharper with increasing doping ratios. which leads to improving the properties of these films. Figure 2 makes it evident that the peaks formed for the polymer films at the ratios (3%, 7%) match the peaks of the CoO NPs nanoparticles shown in Figure 1 at (2θ = 20.3°, 32.2°, 37.84°, 44.81°, 60.4°, and 66.4°). Figure 2 shows the XRD patterns obtained for pure (PVA/PAA) polymer films doped with CoO nanoparticles at weight ratios (3%, 7%).

3.1.2 FESEM Analysis

To know the surface nature and shape of the cobalt oxide (CoONPs) nanopowder prepared by chemical deposition method, The electron microscope examined the produced samples' surface morphology. microscope type (FEI INSPECT F50) using a voltage difference of (40 kV). Figure 3 show the microscopic images of the cobalt oxide (CoONPs) nanopowder calcined at a temperature of (800Cº). Calcined cobalt oxide nanopowder (CoONPs) were represented as dense aggregates of nanoparticles. We notice that the nanopowder is experiencing a change in nanostructure, as well as an increase in crystallinity and granular size. This is because to the elevated calcination the temperature that results in the continued crystalline growth of the granules and their combination, improving the size of the granules [22].

Also, The scanning electron microscope with field emission (FE-SEM) examination was performed On the ready (PVA /PAA) films before and after reinforcing with cobalt oxide (CoONPs)

nanopowder (3%, 7%) at a temperature of (800 C°), Figure 4 shows the microscopic images of the pure films. The images show that the pure (PVA/PAA) film is homogeneous, which is consistent with [23]. When adding cobalt oxide nanoparticles (CoONPs) at a rate of 3%, 7%) at a temperature (800C°), as shown in Figures 5 and 6, the images demonstrate that the polymeric membranes supported by nanoparticles (PVA/PAA: CoONPs) contain many agglomerates dispersed across the surface, since the findings show that the nanoparticles (CoONPs) incline to form dispersed aggregates in nanocomposite membranes [22], [24].

3.1.3 FT-IR Analysis

FTIR analysis of the prepared films was performed to identify the active aggregates by measuring the transmittance spectrum as a wavenumber function in the 500 - 4000 cm-1 range. Figure 7 shows the characteristic infrared spectrum of the (PVA / PAA) films prepared by the solution casting method before and after reinforcement with different weight ratios (pure,1, 3, 5,7 and 9) (wt%) with calcined Nanoparticles of cobalt oxide (CoONPs) when the temperature is 800C°.

Fourier transform infrared (FT-IR) spectra of the PVA/PAA:CoO nanocomposite and pure PVA/PAA composite are displayed in Figure 7. The absorption bands typical of pure (PVA/PAA) are visible in all spectra composite and (PVA/PAA:CoO) nanocomposite (645,838,1062,1242,1704,2923 and 3244) cm^{-1} . It is evident that these treatments result in major variations in the intensity of certain absorption bands as well as certain discernible changes in the samples' spectral characteristics. Defects brought on by the interaction of the nanoparticles and the polymer might be connected to the bands blend which causes the improvement of the polymer properties. All samples showed broad bands at around (3244 cm^{-1}) because of the polymer matrix chain's O-H groups, peaks at (2923 cm^{-1}) are connected to the lengthening of the current (C-H) bond, 1704 cm^{-1} Stretching (C-O) , 1242 cm^{-1} (C-N) Converging, and 1062 cm^{-1} (C-H) bending for PVA/PAA as shown in Figure 7. Moreover, the vibrational peaks in the array (1062-645) cm^{-1} can be credited to (CoO) [26]. Indicating that cobalt oxide nanoparticles are doped within the (PVA /PAA) composite. The results of the experiment shown in Figure 7 after adding (CoO) nanoparticles. Some polymer chains were broken, and other chains were created in its place; these outcomes are comparable to the findings of the researchers [25], [26].

Figure 3: CoONPs powder calcined at 800°C as seen in FE-SEM images.

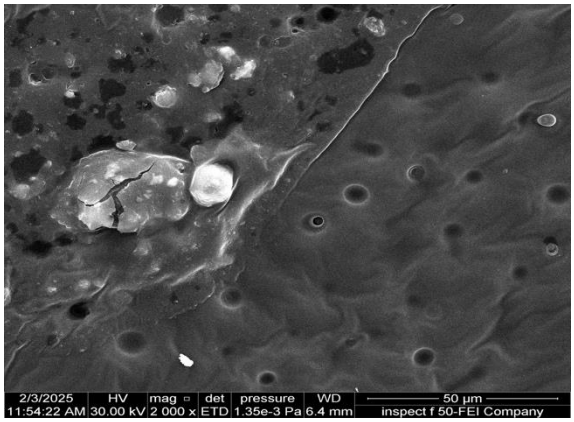

Figure 4: FE-SEM images of pure PVA/PAA films.

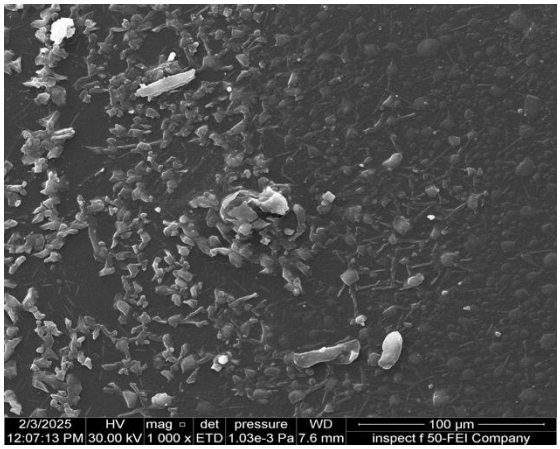

Figure 5: FE-SEM images of films supported by 3% (CoONPs).

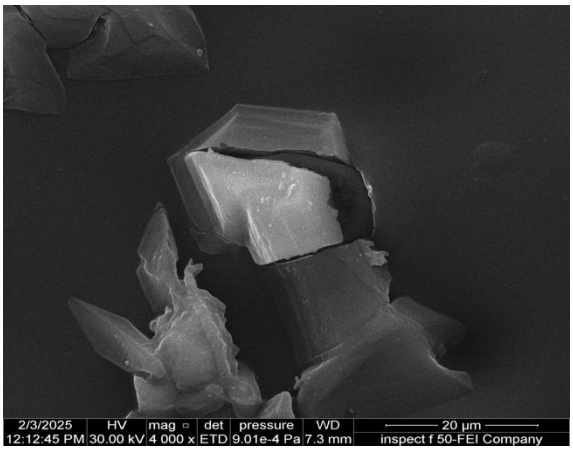

Figure 6 : FE-SEM images of films supported by 7% (CoONPs).

3.2 Optical Analysis

A study of transmittance and absorbance spectra helps in understanding and improving polymer structure and energy bands. Figures 8 and 9 demonstrate the transmittance and absorbance spectrum of the unadulterated mixture (PVA/PAA) and the mixture reinforced with varying weight percentages of burned Nanoparticles of cobalt oxide (CoO NPs) when the temperature is (800 C°). The application of CoO NPs (cobalt oxide nanoparticles) resulted in a decrease in the permeability of the PVA/PAA blend, where the decrease in permeability became more pronounced with the increase in the proportion of CoO NPs. The transmittance of the prepared samples increases with wavelength until it stabilizes at wavelengths above (650-800) nm. This is because increasing the weight ratios of nanoparticles leads to increased nanoparticle density, which in turn leads to increased dispersion and reduced transmittance, according to Reference [27].

On the other hand, The (PVA/PAA) mixture's absorbance rose after the addition of (CoO NPs). In addition, the absorbance decreased significantly with increasing wavelength and stabilized at a wavelength higher than (650-800) nm. This can be ascribed to incident energy being absorbed and dispersed light by (CoO NPs) within the (PVA/PAA) mixture, where part absorbs a portion of the incident light, while the remainder is scattered [28].

The α, the PVA/PAA films' absorption coefficient, was calculated using (2) according to Figure 10. It is demonstrated that the coefficient of absorption of the as-prepared samples is higher at greater photon energies and diminishes with increasing photon energy. The absorption coefficient increases as the content of CoO nanoparticles increases. It is explained by the rise in charge carriers, leading to a higher absorption coefficient of the nanocomposite films. In addition, α is an indicator of the kind of electrical transition found in the films that were developed, as the values of α for PVA/PAA: CoO are [29], [30].

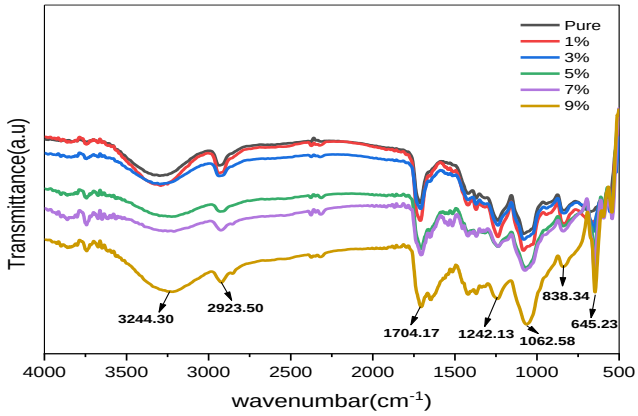

Figure 7: Infrared spectrum of cobalt oxide nanoparticles (CoONPs) calcined at 800 °C and pure (PVA/PAA) films supported with varying weight percentages (pure, 1, 3, 5, 7, and 9) (wt%).

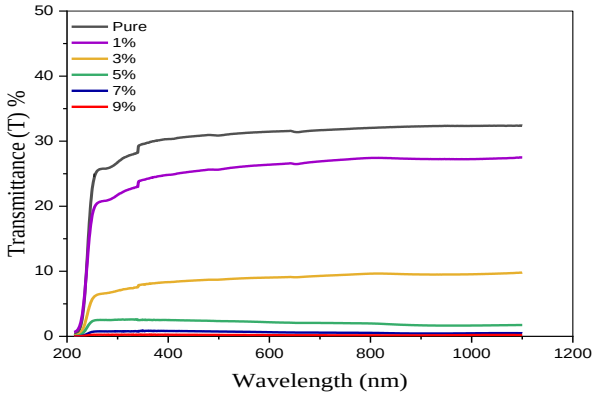

Figure 8: Transmittance spectrum of pure (PVA/PAA) films supported by various weight ratios (wt%) of cobalt oxide nanoparticles (CoONPs) (pure, 1, 3, 5, 7, and 9).

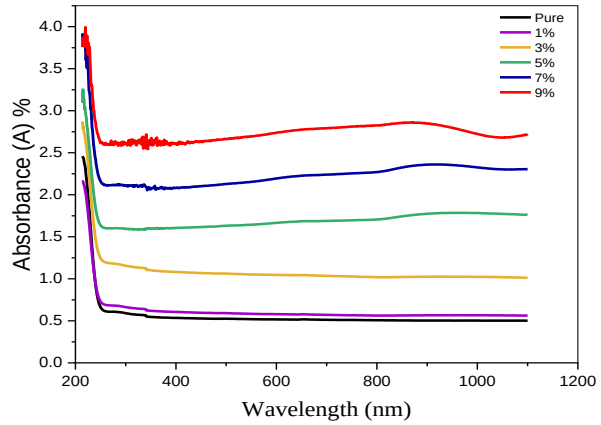

Figure 9: Absorption spectrum of pure (PVA/PAA) films supported by various weight ratios (wt%) of cobalt oxide nanoparticles (CoONPs) (pure, 1, 3, 5, 7, and 9).

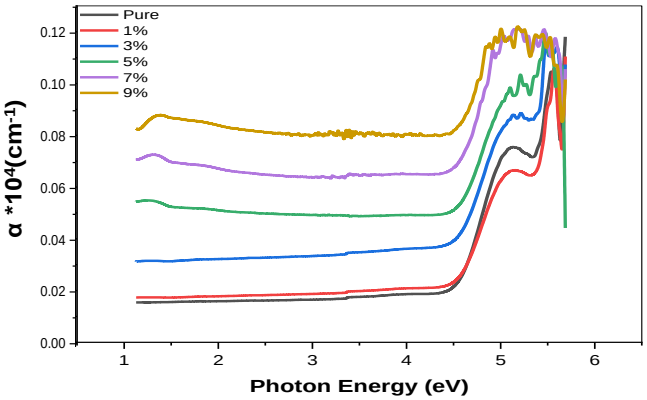

Figure 10: Absorption coefficient for pure (PVA/PAA) films supplemented with varying weight ratios (wt%) of cobalt oxide nanoparticles (CoONPs) (pure, 1, 3, 5, 7, and 9).

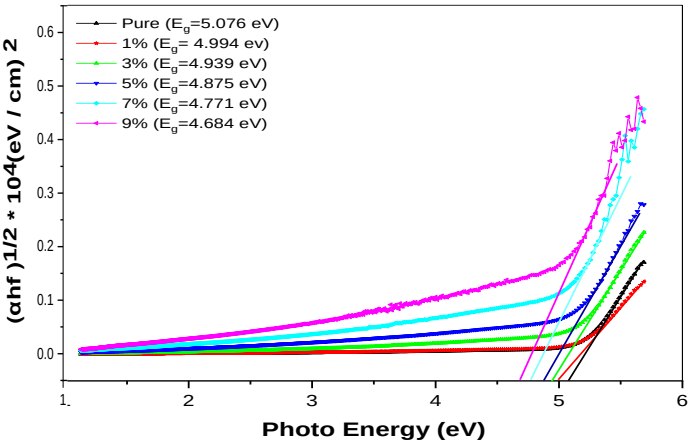

Figure 11: Energy gap for pure (PVA/PAA) films supplemented with varying weight ratios (wt%) of cobalt oxide nanoparticles (CoONPs) (pure, 1, 3, 5, 7, and 9).

As also shown in Figure 11, using pure (3), the energy gap (E_g) value of the PVA-PAA films' indirect electronic transition was determined at 5.076 eV. However, when the amount of cobalt oxide nanoparticles in the reinforced films increases, their E_g values decrease. Upon calcination at 800°C, the values become 4.99 eV, 4.93 eV, 4.87 eV, 4.77 eV, and 4.68 eV for strengthening ratios of (1, 3, 5, 7, and 9) %, respectively. As cobalt oxide (CoO) nanoparticle concentration rises, the defects in the films become more obvious, leading to a reduction in the energy gap measurement. A decrease in energy gap values occurs due to these defects, which generate specific regions of energy levels within them, and the optical properties of the components produced may change as caused by impurities and surface flaws on the nanoparticles that contribute new electrical states [31] .

The index of refraction (n_o) and indicator of extinction (k_o) values of the films PVA / PAA were estimated using (4) and (5). It was observed from Figure 12-13 that as the concentration of (CoO NPs) increased, both (n_o and k_o) increased. (n_o) showed an upward trend, the incident photon energy rises, resulting in an increase in (n_o) for the films that have been prepared. In addition, higher refractive index values with increasing enhancement are due to increased nanoparticle density, also known as packing density. The increase in loss shadow can explain the higher absorption coefficient (α), as there is a strong relationship between the two variables, as agreed by many researchers [27], [32] .

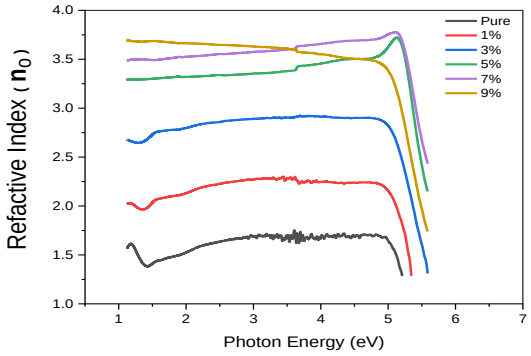

Figure 12: Index of refraction for pure (PVA/PAA) films supported with different wt% (pure,1, 3, 5,7, and 9) of cobalt oxide nanoparticles (CoONP).

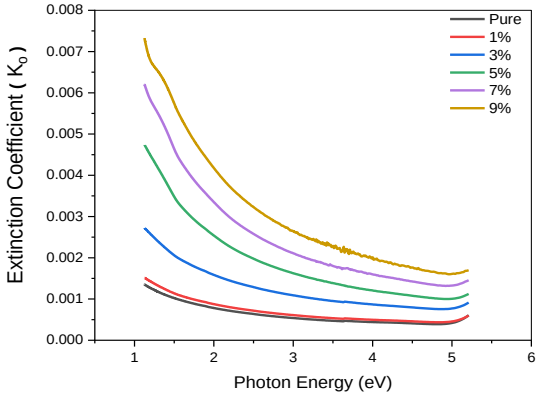

Figure 13: Extinction coefficient for pure (PVA/PAA) films supported with different wt% (pure,1, 3, 5,7, and 9) of cobalt oxide nanoparticles (CoONP).

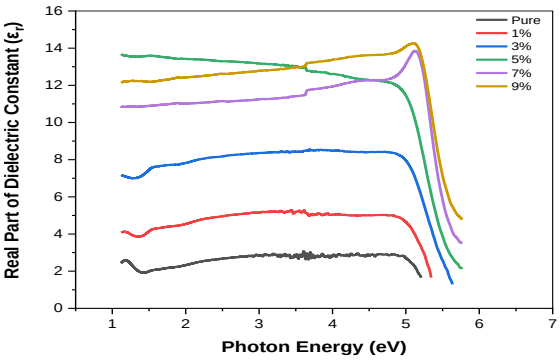

Figure 14: The actual part of pure (PVA/PAA) films supported with different wt% (pure,1,3,5,7and9) of (CoONPs) The temperature at which it was calcined was 800 Cº.

Figures 14-15, which illustrates the change in the real and imaginary parts of the dielectric constant of pure PVA/PAA films supported with varying weight percentages, was calculated using the real portion (ε_r) and the imaginary part (ε_i) of magnesium oxide nanoparticles (CoONPs) as a function of photon energy.

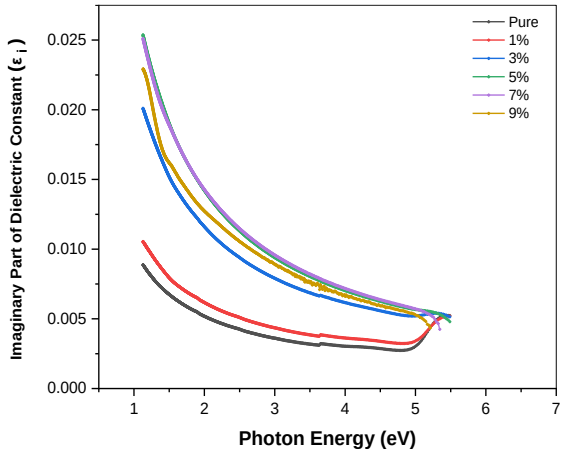

Figure 15: Imaginary part the dielectric constant of pure (PVA/PAA) films supported with different wt% (pure,1,3,5,7and9) of (CoONPs) The temperature at which it was calcined was 800 Cº.

The findings indicate that when calcined cobalt oxide nanoparticles are added to PVA/PAA films, the real and imaginary components of the dielectric constant rise (CoONPs) are added, which is associated with the rise in incoming light absorption and scattering brought on by an increase in nanoparticle proportions [33], [34]. Table 2 displays the energy gap, absorption coefficient, peak extinction coefficient, and peak refractive index values for pure PVA/PAA films that are supported by varying amounts of CoONPs.

Table 2: Values of (energy gap, absorption coefficient, peak refractive index, and peak extinction coefficient) for pure and reinforced (PVA-PAA) films.

Sample	Energy Gap (eV)	(α*10^4 cm^{-1}) Max	(n_o) Max	(k_o) Max
PVA/PAA	5.076	0.024	1.746	0.0013
PVA/PAA: CoONPs (1%)	4.994	0.026	2.306	0.0015
PVA/PAA: CoONPs (3%)	4.939	0.042	2.927	0.0027
PVA/PAA: CoONPs (5%)	4.875	0.054	3.692	0.0047
PVA/PAA: CoONPs (7%)	4.771	0.072	3.706	0.0061
PVA/PAA: CoONPs (9%)	4.684	0.088	3.780	0.0073

4 CONCLUSIONS

The chemical precipitation method has proven effective in Cobalt oxide nanoparticle synthesis, which are used in different weight ratios to enhance the polymer blend (PVA/PAA). The nanocomposite (PVA/PAA:CoONPs) was created using the solution casting method. X-ray diffraction data indicated the effect of calcination temperatures, accompanied by an improvement in crystallinity and crystallite size. FESEM results indicated uniformity, purity, and smoothness of the pure films, but the supported films showed bright spots with agglomerates with high nanoparticle concentration. Visual analysis of the samples indicated that increasing addition of reinforcement is associated with higher values of (A), (α), (n_o), and (ε_r) and (ε_i) components of the dielectric constant, accompanied by a decrease in the values of permeability and energy gap.

We will leverage this research to improve the physical properties of polymer membranes for use in several applications. Future applications: Polymer membranes are used in solar cells, as well as in transistors and medical applications.

REFERENCES

[1] Y. M. Jawad et al., "Fabrication and controlling of physical properties of rhodamine 6G-polystyrene film by low doses of gamma-irradiation," J. Optoelectron. Adv. Mater., vol. 25, pp. 380-386, Jul.-Aug. 2023.

[2] A. M. El Sayed and S. El-Gamal, "Synthesis and investigation of the electrical and dielectric properties of Co3O4/(CMC+PVA) nanocomposite films," J. Polym. Res., vol. 22, p. 97, 2015.

[3] L. Ahmed, B. Zhang, L. C. Hatanaka, and M. S. Mannan, "Application of polymer nanocomposites in the flame retardancy study," J. Loss Prev. Process Ind., vol. 55, pp. 381-391, 2018.

[4] N. S. Alghunaim, "Effect of CuO nanofiller on the spectroscopic properties, dielectric permittivity and dielectric modulus of CMC/PVP nanocomposites," J. Mater. Res. Technol., vol. 8, pp. 3596-3602, 2019.

[5] Q. Xin, Y. Pan, C. Zhang, L. Zhang, C. Dong, L. Lin, L. Zhao, H. Ye, and Y. Zhang, "An exploration of novel natural gas leak detection based on the efficient CH4/N2 separation of polymer blend membrane," Sep. Purif. Technol., vol. 336, p. 126302, 2024.

[6] A. A. Mohammed, A. R. Ahmed, and M. H. Al-Timimi, "Structural, optical and thermal properties of (PEG/PAA:MnO2) nano composites," Tech. Biochem., vol. 3, pp. 107-119, 2022.

[7] A. M. Abdelghany, N. Y. Elamin, Sh. Younis, and D. M. Ayaad, "Polyvinyl pyrrolidone/carboxymethyl cellulose (PVP/CMC) polymer composites containing CuO nanoparticles synthesized via laser ablation in liquids," J. Mol. Liq., vol. 403, p. 124857, 2024.

[8] Y. M. Jawad and M. F. H. Al-Kadhemy, "Enhancement of optical properties of CMC/PAA polymer blend by MgO, SiO2 and bacteriocin for antimicrobial packaging application," J. Glob. Sci. Res., vol. 6, pp. 1715-1725, 2021.

[9] M. M. Damoom, A. Saeed, E. M. Alshammari, A. M. Alhawsawi, A. Y. Yassin, J. A. M. Abdulwahed, and A. A. Al-Muntaser, "The role of TiO2 nanoparticles in enhancing the structural, optical, and electrical properties of PVA/PVP/CMC ternary polymer blend: nanocomposites for capacitive energy storage," J. Sol-Gel Sci. Technol., vol. 108, pp. 742-755, 2023.

[10] M. Roohani, "Cellulose whiskers reinforced polyvinyl alcohol copolymers nanocomposites," Eur. Polym. J., vol. 44, pp. 2489-2498, 2008.

[11] C. C. Demerlis and D. R. Schoneker, "Review of the oral toxicity of polyvinyl alcohol (PVA)," Food Chem. Toxicol., vol. 41, pp. 319-326, 2003.

[12] M. Mahsan, C. Sheng, M. Isa, E. Ali, and M. Razali, "Structural and physical properties of PVA/TiO2 composite," in Malaysia Polymer Int. Conf., pp. 486-495, 2009.

[13] V. G. Kadajji and G. V. Betageri, "Water soluble polymers for pharmaceutical applications," Polymers, vol. 3, no. 4, pp. 1972-2009, 2011.

[14] M. S. Al-Fakeh and R. O. Alsaedi, "Synthesis, characterization, and antimicrobial activity of CoO nanoparticles from a Co(II) complex derived from polyvinyl alcohol and aminobenzoic acid derivative," Sci. World J., p. 11, 2021.

[15] K. A. Dawood et al., "Preparation of polyvinyl alcohol-poly-acrylic acid-cobalt oxide nanoparticles nanocomposites and study their optical properties," Int. J. Sci. Res., vol. 3, no. 12, pp. 276-279, 2014.

[16] Y. M. Jawad et al., "Study the effect of the incorporation of silicon dioxide nanoparticles on improved performance of carboxymethyl cellulose physical characteristics," in AIP Conf. Proc., vol. 2398, no. 1, AIP Publ., 2022.

[17] M. S. Jalil, A. T. Hassan, and Y. M. Jawad, "Investigation of sensitivity of silver-doped tin oxide nanostructures to nitrogen dioxide gas," Iraqi J. Appl. Phys., vol. 19, no. 4B, 2023.

[18] I. R. Agool, K. J. Kadhim, and A. Hashim, "Fabrication of new nanocomposites: (PVA-PEG-PVP) blend-zirconium oxide nanoparticles for humidity sensors," Int. J. Plast. Technol., vol. 21, no. 2, pp. 397-403, 2017.

[19] M. N. J. Al-Delaimi, "The effect of Ni, Cu, CB additives on electrical, optical, and mechanical properties of PMMA," Ph.D. dissertation, Univ. Baghdad, Coll. Sci., 1996.

[20] A. D. A. Buba and J. S. A. Adelabu, "Optical and electrical properties of chemically deposited ZnO thin films," Pac. J. Sci. Technol., vol. 11, no. 2, pp. 429-434, 2010.

[21] S. H. Abead, K. N. Abbas, and M. F. H. Al-Kadhemy, "The structural and optical properties of PVA/CMC copolymer cured by UV irradiation for different times," Emerg. Mater. Res., vol. 13, no. 2, pp. 104–113, Apr. 2024.

[22] N. K. Abbas, M. A. Habeeb, and A. J. K. Algidsawi, "Preparation of chloro penta amine cobalt (III) chloride and study of its influence on the structural and some optical properties of polyvinyl acetate," Int. J. Polym. Sci., pp. 1-10, 2015.

[23] M. Habeeb and A. S. R. Hamza, "Synthesis of (polymer blend-MgO) nanocomposites and studying electrical properties for piezoelectric application," Indonesian J. Electr. Eng. Informat., vol. 6, no. 4, pp. 428-435, 2018.

[24] E. Sheha, H. Khoder, T. S. Shanap, M. G. El-Shaarawy, and M. K. El-Mansy, "Structure, dielectric and optical properties of p-type (PVA/CuI) nanocomposite polymer electrolyte for photovoltaic cells," Optik, vol. 123, p. 13, 2012.

[25] M. Ghanipour and D. Dorranian, "Effect of Ag-nanoparticles doped in polyvinyl alcohol on the structural and optical properties of PVA films," J. Nanomater., 2013.

[26] H. M. M. Al-Tamimi, "Study of some physical properties of (PVA-PAAm-CoO) nanocomposites," J. Univ. Babylon, pp. 62-67, 2014.

[27] A. Mawat, M. Al-Timimi, W. Albanda, and M. Abdullah, "Morphological and optical properties of Mg1-xCdSx nanostructured thin films," vol. 2475, 2023.

[28] A. Hashim and A. M. Habeeb, "Synthesis and characterization of polymer blend-CoFe2O4 nanoparticles as humidity sensors for different temperatures," Trans. Electr. Electron. Mater., vol. 20, no. 2, pp. 107-112, 2019.

[29] I. R. Agool, K. J. Kadhim, and A. Hashim, "Fabrication of new nanocomposites: (PVA-PEG-PVP) blend-zirconium oxide nanoparticles for

humidity sensors," Int. J. Plast. Technol., vol. 21, no. 2, pp. 397-403, 2017.

[30] V. Sangawar and M. Golchha, "Evolution of the optical properties of polystyrene thin films filled with zinc oxide nanoparticles," Int. J. Sci. Eng. Res., vol. 4, no. 6, pp. 2700-2705, 2013.

[31] A. Hashim and Q. Hadi, "Structural, electrical and optical properties of (biopolymer blend/titanium carbide) nanocomposites for low cost humidity sensors," J. Mater. Sci.: Mater. Electron., vol. 29, no. 13, pp. 11598-11604, 2018.

[32] D. Nerkar, S. Panse, S. Patil, S. Jaware, and G. Padhye, "Polypyrrole-silver nanocomposite: synthesis and characterization," 2016.

[33] T. K. Kundu, N. Karak, P. Barik, and S. Saha, "Optical properties of ZnO nanoparticles prepared by chemical method using poly(vinyl alcohol) (PVA) as capping agent," Int. J. Soft Comput. Eng., vol. 1, pp. 19-24, 2011.

[34] H. K. Chitte, N. V. Bhat, N. S. Karmakar, D. C. Kothari, and G. N. Shinde, "Synthesis and characterization of polymeric composites embedded with silver nanoparticles," World J. Nano Sci. Eng., vol. 2, no. 1, pp. 19-24, 2012.